Theoretical premises of thermal wedge effect in fluid-film bearings supplied with a non-homogeneous lubricant

Alexey V. Kornaev, Elena P. Kornaeva and Leonid A. Savin

***Abstract*—**A computational model of a plain fluid-film bearing with means to create artificial thermal and viscosity wedge effect has been developed. The model of fluid film is based on the numerical solution of the generalized Reynolds equation simultaneously with the energy equation. It is assumed, that the lubricant is supplied to the bearing in the form of a mixture of non-homogeneous temperature. Thermal boundary condition on the edge of the bearing is a periodic function, which is characterized by the value of temperature drop and the offset. The governing equations have been solved using finite difference method combined with the iteration procedure. A linearized dynamic model of a rigid symmetric rotor has been used to study lateral vibrations. The results have proven efficiency of application of artificial thermal and viscosity wedges to lightly loaded rotors. It is shown, that a correct choice of the offset value significantly influences the effect of load-carrying capacity's and damping capacity's increase. Vice versa, an incorrect choice of the offset could lead to decrease of load-carrying capacity and result in occurrence of unstable oscillations of a rotor.

***Keywords*—**hydrodynamic lubrication, generalized Reynolds equation, energy equation, thermal and viscosity wedge effect, load-carrying capacity, fluid-film bearing, oil whirl.

I. Introduction

THE main advantage of hydrodynamic lubrication is full separation of surfaces due to generation of load-carrying capacity. However, with the increase of sliding speed friction forces increase at a higher rate than load-carrying capacity. This effect is represented by the right-hand side of the Stribeck curve [1, 2]. Most power losses due to friction occur in bearings of high-speed light load rotor machines.

Three main ways of energy efficiency increase of hydrodynamic lubrication could be highlighted: modernization of design and materials of fluid-film bearings; modernization of lubricants and modernization of operational regimes of bearings. First two approaches could be illustrated by macro [2, 3] and micro-texturing [2, 4, 5], application of porous materials [2, 6], and 'smart' materials. The second approach is based on enhancement of properties of lubricants, generally by means of using additives [2, 7]. Third approach is relatively young and is based essentially on a specific control system [2, 8, 9].

The present paper investigates performance of fluid-film bearings when thermal wedge effect is present to enhance the effect of the hydrodynamic wedge in the film. The research of the thermal wedge effect began with works of Fogg in 1946 and resulted in discovering the possibility to generate load-carrying capacity in a parallel plate thrust bearing [2]. Later this effect was explained by Dowson by thermal expansion of the bearing's parts, and Young in [10] has shown that for high load-carrying capacity large thermal gradients and very thin film are required. Despite this, research in this direction has not stopped [2, 11, 12]. Today, the density wedge and the viscosity wedge are considered separate effects. However, in spite of being always positive, the density wedge effect is insignificant enough to be neglected [2]. The viscosity wedge effect may be positive or negative and could be of the same magnitude as the hydrodynamic effect in a convergent gap [2]. The viscosity wedge may occur not only due to thermal non-homogeneity, but also due to complex rheology. Earlier, in [13] a problem of rheology properties optimization has been considered and was aimed at decreasing the power losses due to friction. A rheological model and a periodic viscosity distribution function, where the maximum is misaligned relatively to the maximum of pressure approximately by quarter of a revolution, have been obtained [13]. However, the model was considered not entirely realistic. In the present paper the problem of artificial thermal wedge generation is investigated by means of supplying the lubricant of non-homogeneous temperature. In comparison to the approach where the same has been implemented by means of non-homogeneous heating of the bearing's parts [2], the

This work was supported by the grant of the President of the Russian Federation No14.Z56.17.1643-MK and by the Russian Science Foundation under the project No16-19-00186 (formulation and solution of a rotor dynamics problem in sections 2, 3 of the present paper).

A. V. Kornaev is with the Modeling of Hydromechanical Systems Research Laboratory at the Orel State University named after I.S. Turgenev, Orel, 302026, Russian Federation (corresponding author to provide e-mail: rusakor@inbox.ru).

E. P. Kornaeva is with the Department of Information Systems at the Orel State University named after I.S. Turgenev, Orel, 302026, Russian Federation (e-mail: lenoks_box@mail.ru).

L. A. Savin is with the Department of Mechatronics and International Engineering at the Orel State University named after I.S. Turgenev, Orel,

present approach is less inertial, allows temperature and viscosity variation in wider ranges, and could be practically implemented by means of controlled sectional supply of lubricant.

II. Mathematical Model

The steady-state flow of a viscous incompressible fluid in a cylindrical fluid-film bearing with diameter D and length L is considered in this study. A rotor with radius r is revolving with a constant speed ω and performs lateral vibrations (Fig. 1). A lubricant is supplied in axial direction due to the pressure drop Δp on bearing's edges. It is assumed, that fluid's temperature is variable, temperatures of the rotor's surface θ_0 and the bearing's surface θ_1 are known and constant. The lubricant is considered Newtonian fluid, viscosity of which is a function of temperature.

The flow area is characterized by the radial gap described using the angular coordinate[1]:

$$h(x_1) = h_0 - X_1 \sin(\alpha) - X_2 \cos(\alpha), \quad (1)$$

where h_0 is the mean oil film thickness; (X_1, X_2) are coordinates of the center of the rotor; $\alpha = x_1 / r$ is the angular coordinate; r is the journal's radius.

For small values of dimensionless Reynolds criterion and small values of geometry criterion $\delta = h_0 / r$, the assumptions made during the derivation of the Reynolds equation are considered justified [1]. The generalized Reynolds equation considers viscosity as a function of space coordinates and changes, among other things, across the film's thickness:

$$\frac{\partial}{\partial x_1}\left[\frac{\partial p}{\partial x_1}\left(F_1 - \frac{f_1}{f_0}F_0\right)\right] + \frac{\partial}{\partial x_3}\left[\frac{\partial p}{\partial x_3}\left(F_1 - \frac{f_1}{f_0}F_0\right)\right] = \frac{\partial}{\partial x_1}\left(\frac{u_1}{f_0}F_0 - u_1 h\right) + u_2, \quad (2)$$

where $p = p(x_1, x_3)$ is pressure function;

$$F_0(x_1, x_3) = \int_0^h \left\{\int_0^{x_2}\left(\frac{dx_2}{\mu}\right)\right\} dx_2,$$

$$F_1(x_1, x_3) = \int_0^h \left\{\int_0^{x_2}\left(\frac{x_2}{\mu}\right) dx_2\right\} dx_2, \qquad f_0(x_1, x_3) = \int_0^h \left(\frac{dx_2}{\mu}\right),$$

$f_1(x_1, x_3) = \int_0^h \left(\frac{x_2}{\mu}\right) dx_2$ are additional functions; $\mu = \mu(x_i)$ is viscosity function $(i = 1...3)$; u_1, u_2 accordingly the tangential and normal components of the rotor's surface's velocity.

A more convenient form of the equation not considering the rotor's vibrations, but considering the change of density across the film's thickness is shown in [1, 14].

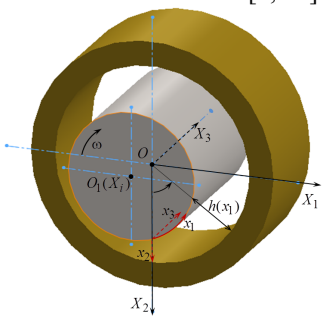

Fig. 1 calculation scheme of a fluid-film bearing

The values of u_i over the surface of the rotor could be determined using the following kinematic relations [1]:

$$\begin{aligned} u_1 &= \omega r + V_1 \cos(\alpha) - V_2 \sin(\alpha), \\ u_2 &= V_1 \sin(\alpha) + V_2 \cos(\alpha), \end{aligned} \quad (3)$$

where $\vec{V} = [\![V_1 \quad V_2 \quad 0]\!]$ is velocity of the center of the rotor.

Calculation of pressure distribution is a boundary problem of solution of the Reynolds equation (2) considering (1), (3) with the following boundary conditions: the pressure on each side of the bearing is known to be $p(x_1, 0) = p_0$ and $p(x_1, L) = p_1$, along the x_1 direction the following periodical condition has to be met $p(0, x_3) = p(\pi D, x_3)$, $\partial p(0, x_3)/\partial x_1 = \partial p(\pi D, x_3)/\partial x_1$. Additionally, the Gumbel's boundary condition for film rupture is used [1].

The energy equation for the studied range of factors' values must take convection and dissipation into account (see Table 1). Given that the relative gap is small, the equation takes the following form [1]:

$$v_1 \frac{\partial \theta}{\partial x_1} + v_3 \frac{\partial \theta}{\partial x_3} = a \frac{\partial^2 \theta}{\partial x_2^2} + \frac{\mu}{2\rho C_p}\left(\left(\frac{\partial v_1}{\partial x_2}\right)^2 + \left(\frac{\partial v_3}{\partial x_2}\right)^2\right) \quad (4)$$

where $\vec{v} = [\![v_1 \quad 0 \quad v_3]\!]$ is the fluid's velocity vector function; θ is the temperature function; a is the heat transfer coefficient; $\mu = \mu(\theta) = b_1\theta + b_2$ is viscosity as a linearized function in the given range of temperatures; C_p is specific heat.

Boundary conditions for equation (4) are presented as follows:

$$\begin{aligned} &\theta(x_1, 0, x_3) = \theta_0, \quad \theta(x_1, h(x_1), x_3) = \theta_1, \\ &\theta(0, x_2, x_3) = \theta(2\pi r, x_2, x_3), \end{aligned} \quad (5)$$

$$\theta(x_1, x_2, 0) = A_\theta \cos\left(\frac{x_1}{r} + \varphi_0\right) + \theta_0. \quad (6)$$

302026, Russian Federation (e-mail: savin@ostu.ru).

[1] Coordinates and velocities of the center of the rotor are indicated with the capital letters, while the coordinates and the velocities of the continuous medium's motion are indicated with the lower case letters.

I Dimensionless criteria range

Dimensionless complex	Order of magnitude
$\delta = \frac{h_0}{r}$	10^{-2}
$Sh = \frac{h_0}{t^* v^*}$	$\le 10^{-4}$
$\mathrm{Re} = \frac{h_0 v^*}{\nu}$	$[10^1;10^2]$
$\mathrm{Pr} = \frac{a}{\nu}$	$[10^2;10^3]$
$Ec = \frac{(v^*)^2}{\rho C_p}$	10^{-3}
$\vartheta = \frac{k h_0 \omega}{v^*}$	10^{-4}

According to (5), a constant temperature is set on the surfaces of the journal and the bearing, and the periodical condition along the circumferential coordinate is met. Inhomogeneous boundary condition (6) is periodic function, which is characterized by the value of temperature drop A_θ and the offset φ_0. The process of determination of pressure distribution, velocities and temperature is iterative. For an initially given temperature distribution the viscosity and pressure distributions (2) are calculated, and, finally, the velocity distribution is calculated:

$$\begin{aligned} v_1^{s+1} &= \frac{\partial p^{s+1}}{\partial x_1} \int_0^{x_2} \frac{x_2}{\mu(\theta^s)} dx_2 + C_1 \int_0^{x_2} \frac{dx_2}{\mu(\theta^s)} + D_1, \\ v_3^{s+1} &= \frac{\partial p^{s+1}}{\partial x_3} \int_0^{x_2} \frac{x_2}{\mu(\theta^s)} dx_2 + C_2 \int_0^{x_2} \frac{dx_2}{\mu(\theta^s)} + D_2. \end{aligned} \quad (7)$$

Unknown functions $C_1(x_1,x_3)$, $C_2(x_1,x_3), D_1(x_1,x_3)$, $D_2(x_1,x_3)$ could be expressed using the kinematic boundary conditions:

$$\begin{aligned} v_1|_{x_2=0} &= u_1, \quad v_2|_{x_2=0} = u_2, \quad v_3|_{x_2=0} = 0, \\ v_1|_{x_2=h(x_1)} &= 0, \quad v_2|_{x_2=h(x_1)} = 0, \quad v_3|_{x_2=h(x_1)} = 0. \end{aligned}$$

Then, a new temperature distribution is calculated (4). The procedure continues until the necessary accuracy is achieved. The value of mean squared error of viscosity distribution before and after the iterative procedure is taken as means of evaluation of accuracy.

Given the pressure distribution, the components of the resulting force on the surface of the rotor can be obtained as projections on the X_i (Fig. 1) [1]:

$$\begin{aligned} R_1 &= -\int_0^L \int_0^{\pi D} p(x_1,x_3)\cos(\alpha) dx_1 dx_3, \\ R_2 &= -\int_0^L \int_0^{\pi D} p(x_1,x_3)\sin(\alpha) dx_1 dx_3. \end{aligned} \quad (8)$$

Another important integral characteristic is the resulting friction torque [1]:

$$M = \int_0^L \int_0^{\pi D} \left(\mu \frac{\partial v_1}{\partial x_2} \right)\Big|_{x_2=0} r dx_1 dx_3 . \quad (9)$$

The equation of lateral vibrations of the center of mass of a rotor can be presented as follows [1, 11-13]:

$$m\, d\vec{V}/dt = \vec{R} + \vec{F} , \quad (10)$$

where m is the mass of the rotor per one bearing; t is time; $\vec{F} = m\Delta\omega^2 \begin{bmatrix} \cos\omega t \\ \sin\omega t \end{bmatrix} + m \begin{bmatrix} 0 \\ -g \end{bmatrix}$ is the bearing load; $m\Delta$ is the rotor's imbalance, g is free fall acceleration.

The approach to linearization of the reaction forces of the lubricant film [1, 15-17] is widely used and is based on the decomposition of reaction force components R_i into the Taylor series in close proximity to the equilibrium position X_i^E. The equilibrium position corresponds to a point where the reaction forces of the film are equal to the rotor's weight. The equilibrium point shall be determined beforehand. Then, the matrices of stiffness and damping could be introduced:

$$K_{ij} = -\left(\frac{\partial R_i}{\partial X_j} \right)\Big|_{\substack{\vec{X}=\vec{X}^E \\ \vec{V}=0}}, \quad B_{ij} = -\left(\frac{\partial R_i}{\partial V_j} \right)\Big|_{\substack{\vec{X}=\vec{X}^E \\ \vec{V}=0}} . \quad (11)$$

Then, the motion equation of the rotor (10) with given conditions of the rotor system's operation and given the linearized reaction forces, will be as follows [1, 15-17]:

$$\begin{aligned} m \begin{bmatrix} dV_1/dt \\ dV_2/dt \end{bmatrix} &= \begin{bmatrix} R_1^E \\ R_2^E \end{bmatrix} - \begin{bmatrix} K_{11} & K_{12} \\ K_{21} & K_{22} \end{bmatrix} \cdot \begin{bmatrix} X_1 - X_1^E \\ X_2 - X_2^E \end{bmatrix} - \\ &- \begin{bmatrix} B_{11} & B_{12} \\ B_{21} & B_{22} \end{bmatrix} \cdot \begin{bmatrix} V_1 \\ V_2 \end{bmatrix} + m\Delta\omega^2 \begin{bmatrix} \cos\omega t \\ \sin\omega t \end{bmatrix} + m \begin{bmatrix} 0 \\ -g \end{bmatrix}. \end{aligned} \quad (12)$$

The initial conditions for equation (10) are: $X_i = X_i^E$, $V_i = 0$. Equations (2) and (4) have been solved numerically using the finite difference method. The obtained set of linear equations was solved using the Gauss method [18]. The

dynamic problem based on the numerical solution of equation (12) has been solved using the explicit Runge-Kutta method of 4th and 5th order [18]. The simulation model based on the developed mathematical model was programmed using GNU-Octave [19].

III. Results and Discussion

Further investigation is based on numerical tests of a rotor-bearing system with the following parameters. One of the rotors of 3.67 kg or 0.367 kg mass rotates at constant speed of 1000 rpm under gravity load and centrifugal force caused by rotor's imbalance $\Delta \cdot m = 4 \cdot 10^{-4}$ kg·m and is supported by two plain radial fluid-film bearings with 40 mm diameter, 10 mm length with mean radial gap of 100 μm. The pressure on each side of the bearing is known to be $p(x_1,0)=0.4$ MPa and $p(x_1,L)=0.1$ MPa. Lubricant is mineral oil "I-12A". Bearing's surface temperature is constant $\theta_0 = 40\,^{O}$C. Supply temperature of the lubricant is described with (6) with a drop value $A_\theta = 10\,^{O}$C and various values of offset $\varphi_0 = 0,-\pi/2,-\pi,-3\pi/2$. The numerical solution was obtained on a $n_1 \times n_2 \times n_3$ grid (indexes correspond to the axes x_i) of $21\times11\times21$ elements.

In the Figure 2 the viscosity measurement results are presented for the 'I-12A' oil with different temperature. The results were obtained using the viscometer "Rheotest RN 4.1" at a constant shear rate $\xi_{12} = 6.58 \cdot 10^3$ 1/s is the maximum speed for this particular viscometer. With the speed of rotor 1000 rpm, the values of shear rate in the fluid film of the studied bearing are of same order of magnitude. Additional tests show, that viscosity of the 'I-12A' oil does not depend significantly on the shear rate and changes by no more than 2% in the whole range of viscometer's speed. Experimental results of viscosity measurement were approximated using a linear and an exponential function (see Figure 2). The mean error was 0.51 Pa·s and 0.15 Pa·s in cases of linear and exponential approximations accordingly. Here, the error of the linear approximation in comparison to the exponential did not exceed 3.4% in the given range of temperatures. So, in the future calculations the linear model of viscosity was used: $\mu(\theta) = -6.56 \cdot 10^{-4}\theta + 4.72 \cdot 10^{-2}$ Pa·s (Fig. 2).

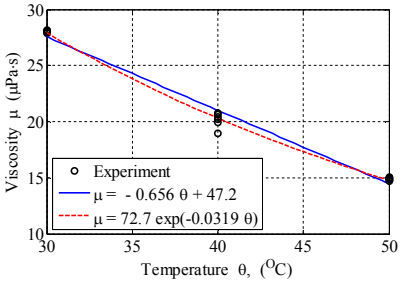

Fig.2 viscosity of oil as a function of temperature

The first series of numerical experiments was carried out in order to study the steady-state regime without lateral vibrations $V_i = 0$ and with given rotor's location $X_1 = -(0.01...0.75)h_0$, $X_2 = 0$ (see Figure 1). The solution was determined out of 2-5 iterations with monotonous decrease of mean error until the accuracy condition is met with order of magnitude of $10^{-3}...10^{-2}\,^{O}$C. The results of test calculations of velocity, pressure and temperature distribution with $X_1 = -0.741h_0$ are shown in the Figures 3, 4. This position corresponds to the equilibrium location when rotor's mass is 3.67 kg. In the Figure 3 the iteration process is presented. The values of mean error of pressure and temperature rapidly decrease to values of 10^{-4} Pa and $10^{-8}\,^{O}$C order of magnitude accordingly at the fifth iteration. A significant influence on the convergence has the geometry parameter L/D. With $L/D \le 0.25$ the solution reaches convergence quite fast. A known fact has to be noted, that the value of the criterion $L/D \le 0.25$ provides stability of the solution of the rotor dynamics problems [1].

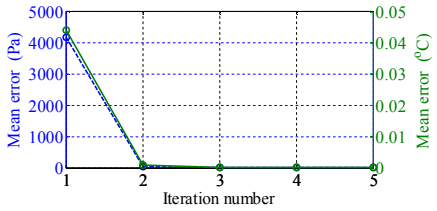

Fig.3 iteration process

The obtained temperature distribution is practically uniform in the flow region due to the type of the thermal boundary conditions (5) (see Figure 4). These are boundary conditions of first order that could be physically interpreted as conditions for heat exchange with a massive high heat capacity body [1, 20, 21].

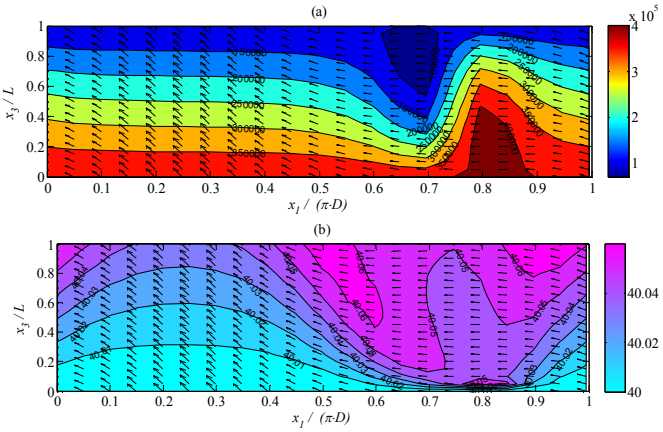

Fig.4 numerical test results with homogeneous boundary conditions (6) $A_\theta = 0$, $\varphi_0 = 0$: pressure (a) and temperature (b) distribution in the $x_2 = h/2$ cross-section in contour lines and velocity distribution in the form of a vector distribution

Figure 5 presents the numerical results of velocity and temperature distribution calculations with various parameters of periodic thermal boundary conditions (6). Thermal conditions of lubricant's supply have been chosen so, that the maximum temperature is located in the convergent part of the radial gap (see Figure 5, (a), (d)), around the area of minimum film thickness (see Figure 5, (b)), or in the divergent part of the gap (see Figure 5, (c)). It could well be seen from the results, that a non-homogeneous flow spreads along the length of the bearing, and the fluid cannot fully warm up (cool down) due to the thermal contact with solid bodies.

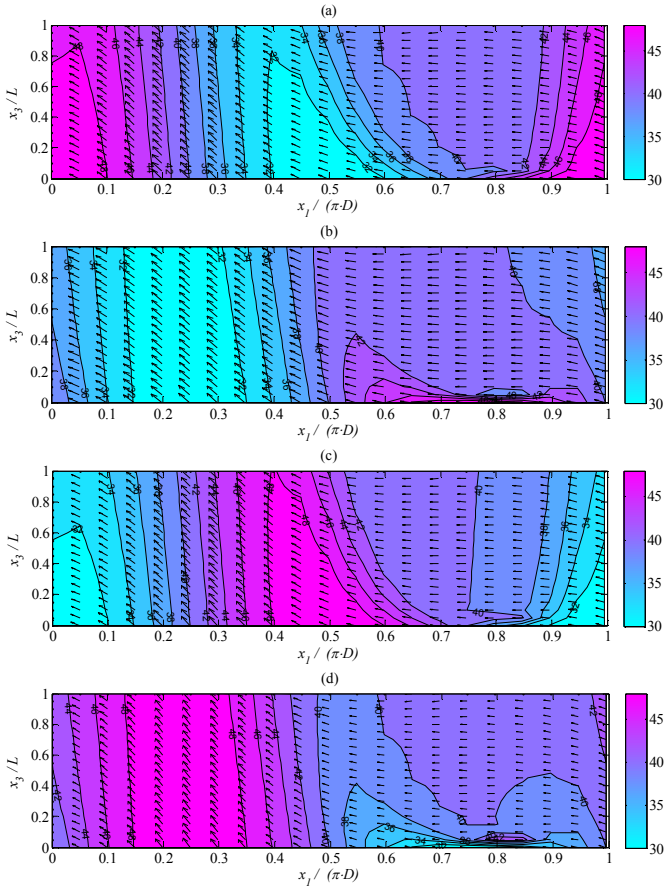

Fig. 5 vector distribution of velocity and contour temperature distribution in the $x_2 = h/2$ cross-section with various parameters of periodic thermal boundary conditions (6): $A_\theta = 10$, $\varphi_0 = 0$ (a), $A_\theta = 10$, $\varphi_0 = -\pi/2$ (b), $A_\theta = 10$, $\varphi_0 = -\pi$ (c), $A_\theta = 10$, $\varphi_0 = 3\pi/2$ (d).

Figure 6 shows the numerical results of calculation of basic integral characteristics. First of all, the presence of artificial thermal wedge resulted in occurrence of a horizontal component of the resulting force R_1, value of which does not significantly depend on eccentricity, but is rather dependent on the offset φ_0, this could be observed in the Figure 6 (a). When $\varphi_0 = -\pi/2$ and $\varphi_0 = -\pi$, i.e. when the hottest flow is in the minimum film thickness area or in the divergent area after it, the component R_1 is directed towards the center of the bearing, which should affect the rotor dynamics positively. The positive effect for the vertical component of the resulting force R_2 has shown when $\varphi_0 = 0$ and $\varphi_0 = -3\pi/2$, i.e. when the hottest flow is in the area of a converging gap (see Figure 6 (b)). The thermal wedge has not affected the friction torque significantly in any of the studied cases (see Figure 6 (c)). Figure 6 (d) shows the values of a conditional friction coefficient $f = M/(rR)$. The friction coefficient decreased the most in case of $\varphi_0 = 0$ and hottest flow in the converging gap in proximity to the minimum film thickness. This result is consistent with the results of viscosity distribution optimization by the criterion of minimum power losses due to friction in [3]. In all cases of $A_\theta \neq 0$ presence of the thermal wedge significantly decreased the friction coefficient with low eccentricities $e/h_0 \leq 0.1$. For instance, in the studied bearing with relative eccentricity $e/h_0 = 0.1$, the friction coefficient could be decreased by four times.

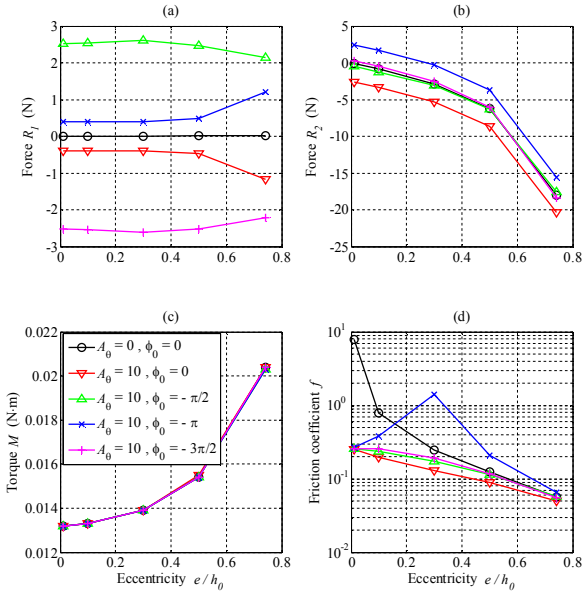

Fig. 6 integral characteristics calculation results of a fluid-film bearing with constant rotor's speed $n = 1000$ rpm and various values of relative eccentricity e/h_0: projection of the resulting force in the film on the horizontal (a) and vertical (b) axes; friction torque (c) and friction coefficient (d)

The second series of numerical experiments considered the study of rotor's oscillations around the equilibrium position. Pressure distribution calculation was again implemented in 2-5 iterations with monotonous decrease of the mean squared error. In the Figure 7 (a) the trajectories of a heavier rotor's

oscillations are presented, with rotor's mass 3.67 kg and relative eccentricity $e/h_0 \approx 0.75$. In the Figure 7 (b) the oscillations of a lighter rotor are presented, with rotor's mass 0.367 kg and relative eccentricity $e/h_0 \approx 0.2$. It could be seen from the trajectories' shape, that supply of a hotter lubricant to the convergent area of the gap leads to a decrease in damping capacity of the film. In some cases, the dynamic behavior of the rotor becomes unstable, which could result in mixed or boundary lubrication and lead to increased wear and failure of the bearing [1,2]. In order to quantitively analyze the rotor dynamics, the frequency responses have been obtained (Fig. 8).

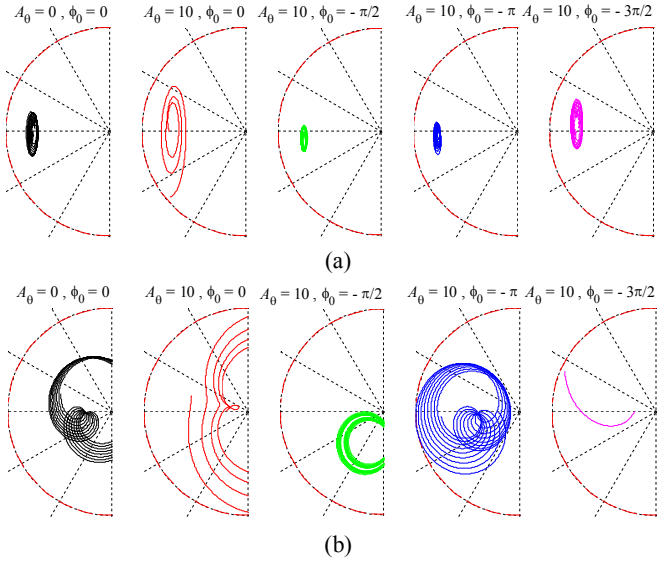

Fig.7 rotor's oscillations simulation results for various boundary conditions (6): case of a relatively heavy rotor 3.67 kg (a) and a relatively light rotor 0.367 kg (b)

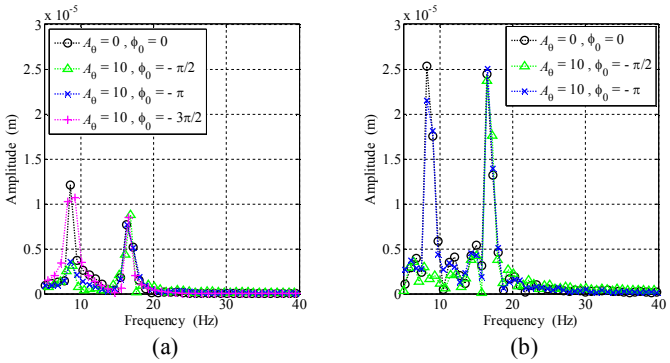

Fig.8 numerical results of frequency response of rotor's oscillations calculation with various thermal boundary conditions (6): in case of a relatively heavy rotor 3.67 kg (a) and relatively light rotor 0.367 kg (b)

It could be observed from the results, that the oscillations are characterized by two harmonics. The frequency of the first harmonic corresponds to approximately half the rotational speed. This is a typical of half-speed oil whirl [1, 16, 17]. The second harmonic corresponds to the rotational frequency, and the centrifugal force causes oscillations. In case of $\varphi_0 = -\pi/2$ supply of hot lubricant directly into the area of minimum film thickness, a more significant decrease of oscillations' amplitude takes place regarding the first harmonic, which could not only be observed in the Figure 8, but also in the Figure 7. So, generation of a thermal wedge with maximum temperature in the area of minimum film thickness could allow decreasing power losses due to friction and vibration level in fluid-film bearings.

IV. Conclusions

Based on the presented results of numerical experiments a conclusion could be drawn, that generation of a thermal wedge by means of supplying a lubricant of non-homogeneous temperature possibly provides conditions to decrease power losses due to friction and level of vibrations in a fluid-film bearing. The viscosity wedge effect occurs due to the change in viscosity in the direction of flow, which results in generation of additional hydrodynamic force. The value of this force is determined by the properties of a fluid, temperature drop's value in circumferential direction, pressure drop's value in axial direction and dimensions of a bearing. However, the additional force practically does not depend on eccentricity, so it does not disappear even if a rotor is located coaxially in a bearing. Direction of the additional hydrodynamic force is determined by the location of a thermal wedge. Generation of an additional component of the reaction force of the fluid film helps minimize self-excited oscillations in a bearing, only if the maximum of a thermal wedge is located around the area of minimum film thickness. The most vivid effect of a thermal and viscosity wedges could be observed when lubricating fluid-film bearings with small eccentricity, i.e. the bearings which have conditionally excessive load-carrying capacity.

Further study is based on the development of the simulation model and the development of a test rig where a lubricant is supplied to the bearing in the form of a mixture of non-homogeneous temperature. It is promising to use complex rheology lubricants to enhance the effect of the viscosity and thermal wedges. The obtained results could be used while developing lightly loaded rotor-bearing systems in which the question of energy efficiency is of highest importance, e.g. industrial pumps for viscous fluids and compact rotor systems in medicine and instrumentation.

Acknowledgment

The authors thank Alexander Fetisov for carrying out the experiment with viscosity measurement and to Alexander Babin for the translation.

AUTHOR CONTRIBUTIONS

Alexey Kornaev and Elena Kornaeva developed the fluid flow mathematical model, script the simulation program and wrote the manuscript. Alexey Kornaev and Leonid Savin developed rotor dynamics mathematical model and analyzed the numerical experiment's results. Leonid Savin was in charge of supervising this work.

REFERENCES

[1] Hori, Y. *Hydrodynamic Lubrication*, Yokendo Ltd: Tokyo, 2006.

[2] *Encyclopedia of Tribology;* Edited by Q.J. Wang and Y.-W. Chung, Springer: New York, 2013.

[3] Charitidis, C.A.; Koumoulos, E.P.; Dragatogiannis, D.A. "Nanotribological behavior of carbon based thin films: friction and lubricity mechanisms at the nanoscale," *Lubricants* 2013, *1*, 22-47, DOI: 10.3390/lubricants1020022.

[4] Henry, Y.; Bouyer, J.; Fillon, M. "An experimental analysis of the hydrodynamic contribution of textured thrust bearings during steady state operation – comparison with the untextured parallel surface configuration," *Proceedings of the Institution of Mechanical Engineers Part J Journal of Engineering Tribology,* vol. 229, pp. 362-375, 2015.

[5] Dadouch, A.; Conlon, M.J. "Operational performance of textured journal bearings lubricated with a contaminated fluid," *Tribol. Int.,* vol. 93, pp. 377 – 389, 2016, http://dx.doi.org/10.1016/j.triboint.2015.09.022.

[6] Balasoiu, A.M.; Braun, M.J.; Moldovan, S.I. "A parametric study of a porous self-circulating hydrodynamic bearing," *Tribol. Int.*, vol. 93, pp. 176 – 193, 2013, http://dx.doi.org/10.1016/j.triboint.2012.12.015.

[7] Brito, F.P.; Miranda, A.C.; Clario, J.C.P.; Teixeira, J.C.; Costa, L.; Fillon, M. "The role of lubricant feeding conditions on the performance improvement and friction reduction of journal bearings," *Tribol. Int.,* vol. 72(4), pp. 65 – 82, 2014.

[8] Eling, R.; Wierik, M; Ostayen, R.; Rixen, D. "Towards accurate prediction of unbalance response, oil whirl and oil whip of flexible rotors supported by hydrodynamic bearings," *Lubricants,* vol. 4, pp. 18, 2016, DOI: 10.3390/lubricants4030033.

[9] Polyakov, R.; Shutin, D.; Savin, L.; Babin, A. "Peculiarities of reactions control for rotor positioning in in an active journal hybrid bearing," *International Journal of Mechanics,* vol. 10, pp. 62-67, 2016.

[10] Young, J. "Thermal wedge effect in hydrodynamic lubrication," *The Engineering Journal*, vol. 45, pp. 46–54, 1962.

[11] Lebeck, A. "Parallel sliding load support in the mixed friction regime," Part 2 - Evaluations of the mechanisms. *Journal of Tribology,* vol. 109, pp. 196-205, 1987.

[12] Meng, Xi; Khonsari, M.M. "On the effect of viscosity wedge in micro-textured parallel surfaces," *Tribol. Int.,* vol. 107, 116 – 124, 2017, http://dx.doi.org/10.1016/j.triboint.2016.11.007.

[13] Savin, L.; Kornaev, A.; Kornaeva, E. "Effect of lubrication of fluid friction bearings with media of complex rheology," *Applied Mechanics and Materials*, vol. 630, pp. 199-207, 2014, DOI:10.4028/www.scientific.net/AMM.630.199.

[14] Dowson, D. "A generalized Reynolds equation for fluid-film lubrication," *International Journal of Mechanical Sciences*, vol. 4(2), 159-170*,* 1962, DOI: 10.1016/S0020-7403(62)80038-1.

[15] Kornaev, A.; Kornaev, N; Kornaeva, E. "Calculation of rotor trajectories using neural network program module (Periodical style—Accepted for publication)," *International Journal of Rotating Machinery,* to be published.

[16] Childs, D. *Turbomachinery Rotordynamics. Phenomena, Modeling and Analysis*, John Wiley&Sons: New York, 2010.

[17] Yamamoto, T. *Linear and Non-Linear Rotordynamics. A Modern Treatment with Applications*, John Wiley&Sons: New York, 2001.

[18] Salvadori, M.G.; Baron, M.L. *Numerical Methods in Engineering,* 2nd ed.; Prentice-Hall: Englewood Cliffs, N.J., 1961.

[19] GNU Octave [Online]. Available: http://www.gnu.org/software/octave (accessed on 30 December 2016).

[20] Milne-Thomson, L.M. *Theoretical Hydrodynamics,* Macmillan & Co. Ltd.: London, UK, 1962.

[21] Boncompain, R.; Fillon, M.; Frene, J. "Analysis of thermal effects in hydrodynamic bearings," *Journal of Tribology,* vol. 108, 108, 219-224, 1986.